Lithium promotes recovery after spinal cord injury

Ying-Jie Zhao[1], Hao Qiao[1], Dong-Fan Liu[1], Jie Li[1], Jia-Xi Li[1], Su-E Chang[1], Teng Lu[1], Feng-Tao Li[1], Dong Wang[1], Hao-Peng Li[1], Xi-Jing He[1, 2, *], Fang Wang[1, *]

From the Contents

Graphical Abstract *Proposed mechanisms of lithium-mediated protection against spinal cord injury (SCI) and promotion of nerve repair after SCI*
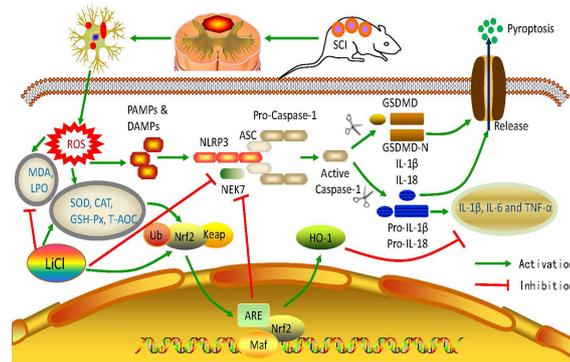
Abstract

Lithium is associated with oxidative stress and apoptosis, but the mechanism by which lithium protects against spinal cord injury remains poorly understood. In this study, we found that intraperitoneal administration of lithium chloride (LiCl) in a rat model of spinal cord injury alleviated pathological spinal cord injury and inhibited expression of tumor necrosis factor α, interleukin-6, and interleukin 1 β. Lithium inhibited pyroptosis and reduced inflammation by inhibiting Caspase-1 expression, reducing the oxidative stress response, and inhibiting activation of the Nod-like receptor protein 3 inflammasome. We also investigated the neuroprotective effects of lithium intervention on oxygen/glucose-deprived PC12 cells. We found that lithium reduced inflammation, oxidative damage, apoptosis, and necrosis and up-regulated nuclear factor E2-related factor 2 (Nrf2) and heme oxygenase-1 in PC12 cells. All-trans retinoic acid, an Nrf2 inhibitor, reversed the effects of lithium. These results suggest that lithium exerts anti-inflammatory, anti-oxidant, and anti-pyroptotic effects through the Nrf2/heme oxygenase-1 pathway to promote recovery after spinal cord injury. This study was approved by the Animal Ethics Committee of Xi'an Jiaotong University (approval No. 2018-2053) on October 23, 2018.
Key Words: anti-inflammatory; anti-oxidant; anti-pyroptosis; cell death; inflammatory factors; lithium; neurons; neuroprotective; Nrf2/HO-1; spinal cord injury

Chinese Library Classification No. R453; R744; Q614.111

Introduction

Many treatment methods are available for spinal cord injury (SCI) in adult patients, such as cell transplantation and methylprednisolone (Assinck et al., 2017; Gazdic et al., 2018). However, the effects of these treatments on SCI repair remain controversial, and they may have some side effects. SCI involves not only the primary physical damage to the spinal cord, but also secondary damage characterized by further neuronal and glial cell injury (Dixon, 2017). The cascade of secondary damage results in serious functional deficits on the injured side (Mortezaee et al., 2018). Pyroptosis is a specific and recently described form of programmed cell death (de Rivero Vaccari et al., 2014; Tsuchiya, 2020). The concept of the inflammasome was first outlined by Xue et al. (2015). NOD-like receptor is a receptor protein (Martinon et al., 2009). The NLRP3 inflammasome is the most widely studied inflammasome. It is activated by recognition of damage- or pathogen-associated molecular patterns (Zhaolin et al., 2019). Once inflammatory receptors are activated, they recruit ASC and pro-Caspase-1 to the inflammasome, inducing cleavage of pro-Caspase-1 into activated Caspase-1. Activated Caspase-1 cleaves Gasdermin-d (GSDMD) directly, releasing the active N-terminal subunit, which in turn cleaves the pro-IL-1β and pro-IL-18 to produce the corresponding cell inflammatory factors IL-1β and IL-18. Ultimately, this cascade induces inflammatory cell death, or pyroptosis (Wu et al., 2020). Pyroptosis is mainly mediated by Caspase-1 and GSDMD, accompanied by the production of various pro-inflammatory mediators such as interleukin (IL)-1β and IL-18 (Broz and Dixit, 2016). The destruction of nerve cells that occurs during the primary SCI activates the inflammasome pathway, further promoting pyroptosis and resulting in the release of inflammatory factors that cause a secondary inflammatory reaction (Kaushal et al., 2015).

[1]Department of Orthopedics, the Second Affiliated Hospital of Xi'an Jiaotong University School of Medicine, Xi'an, Shaanxi Province, China; [2]Department of Orthopedics, Xi'an International Medical Center Hospital, Xi'an, Shaanxi Province, China
*Correspondence to: Xi-Jing He, PhD, MD, xijing_h@vip.tom.com; Fang Wang, MD, wfcn664845753@126.com.
https://orcid.org/0000-0002-1873-7807 (Ying-Jie Zhao); https://orcid.org/0000-0002-0465-5376 (Xi-Jing He); https://orcid.org/0000-0003-4344-7905 (Fang Wang)

Along with the inflammatory response, anabatic oxidative stress also plays a role in the secondary damage that occurs after SCI (Wang et al., 2009a). After SCI, many oxygen radicals are produced, which enhances the oxidative stress response at the site of the lesion (Smith et al., 2012; Li et al., 2014a, b), followed by pathological changes including myelin loss, ongoing pyroptosis along with apoptosis, and interrupted axonal tracts. Glutathione peroxidase (GSH-Px), superoxide dismutase (SOD), catalase (CAT), total antioxidative capacity (T-AOC), malondialdehyde (MDA), and lipid peroxide (LPO) are the main oxidative stress response factors that are activated by SCI. GSH-Px catalyzes H_2O_2 decomposition, reflecting the body's ability to scavenge oxygen free radicals (Kalayci et al., 2005). SOD is the main free radical scavenger in cells and reduces the damage caused by oxygen free radicals (Gökce et al., 2016). CAT promotes the decomposition of H_2O_2 into molecular oxygen and water to prevent cell peroxidation (Jalali et al., 2016). T-AOC levels correlate with the body's overall ability to scavenge free radicals. MDA activity directly reflects the level of oxygen free radicals in the body and indirectly reflects the degree of damage caused to tissues or cells by free radicals (Yuksel et al., 2016). LPO indirectly reflects the content of natural anti-oxidants in tissues and the activity of anti-oxidant enzymes. Among all of the signaling pathways that are associated with anti-oxidant activity, we are especially interested in the nuclear factor E2-related factor 2/heme oxygenase-1 (Nrf2/HO-1) pathway (Ma, 2013). Nrf2 is generally bound to the cytoplasmic retention factor Kelch-like ECH-associated protein 1 (Keap1), which is degraded in response to nerve damage and elevated levels of reactive oxygen species (ROS).

Briefly, Nrf2 translocates to the nucleus, where it promotes the transcription of genes containing an anti-oxidant response element, such as those encoding the Nrf2/HO-1 downstream effector molecules GSH and SOD, thereby activating the Nrf2/HO-1 pathway (Zhai et al., 2013; Xu et al., 2014a; Dwivedi et al., 2016). Its core role as an anti-oxidant has been confirmed by a large number of studies (Ji et al., 2017). Hence, activating the Nrf2/HO-1 pathway can inhibit oxidative stress and subsequent pyroptosis-related signaling cascades. Furthermore, we hypothesize that suppression of pyroptosis and oxidative stress could be potent strategy for therapeutic intervention for SCI in the future.

Lithium is a first-line drug used for bipolar disorder that plays a neuroprotective role in multiple neurological diseases, such as Parkinson's disease (Guttuso, 2019; Gu et al., 2020; Haupt et al., 2021), Huntington's disease (Serafini et al., 2016), and amyotrophic lateral sclerosis (Pasquali et al., 2009). Although one clinical trial showed no significant improvement in patients with SCI treated with lithium (Yang et al., 2012), this study focused on chronic SCI instead of evaluating earlier stages in SCI when therapy is more effective. The acute phase of SCI is critical period for repair, and inflammation is the key to the acute phase, because it determines the extent of recovery from SCI (Ahuja et al., 2017; Anjum et al., 2020).

Several lines of evidence suggest that lithium works through a variety of complex mechanisms, including neuroprotection, induction of neurotrophic factor secretion, neurogenesis, and inhibition of inflammation (Rowe and Chuang, 2004; Rybakowski et al., 2018). Recently, increasing attention has been paid to inhibiting inflammation after lithium treatment. Many animal studies have shown that lithium has great potential for the treatment of acute-phase SCI (Yick et al., 2004; Zakeri et al., 2014; Liu et al., 2017; Tong et al., 2018; Abdanipour et al., 2019).

Although more studies are needed to clarify the full benefits of lithium treatment, this therapeutic option has great potential for the treatment of SCI. One study has identified a connection between lithium treatment and oxidative stress (Xiang et al., 2020). There is also some evidence of a connection between pyroptosis and lithium treatment. However, it remains unknown whether there is a connection between lithium treatment and pyroptosis in SCI and, to date, no study has investigated the effects of lithium on the Nrf2/HO-1 pathway after SCI. In this study, we investigated the effects of, as well as the underlying mechanism of, lithium treatment on acute-phase SCI in rats in terms of oxidative stress, pyroptosis, and the Nrf2/HO-1 pathway.

Materials and Methods

Animals
It is difficult to control the level of estrogen (e.g., as a hormone related to pregnancy, during birth), and female hormone levels have a substantial influence on many experimental results (Pabon et al., 2014; Brotfain et al., 2016; Sircar, 2019). A total of 108 healthy adult male specific pathogen-free Sprague-Dawley rats, weighing 220–250 g, aged 2 months, were used in this study. These animals were provided by the Experimental Animal Center of Xi'an Jiaotong University of China (license No. SCXK (Shaan) 2007-001). This study was performed after the animals had been allowed to acclimatize to the housing facility conditions for 1 week (temperature 20–24°C, humidity 50–70%, 12/12-hour light/dark cycle). All experiments were approved by the Animal Care and Use Committee of Xi'an Jiaotong University (approval No. 2018-2053) on October 23, 2018. All experiments were designed and reported according to the Animal Research: Reporting of *In Vivo* Experiments (ARRIVE) guidelines. The rats were randomly divided into three groups: lithium (SCI + lithium), SCI, and sham (*n* = 36 rats in each group).

Preparation of the spinal cord injury model
A rat model of SCI was established according to a modified Allen's method (Allen, 1911). First, rats were anesthetized by intraperitoneal injection of 3% pentobarbital sodium (1.5 mL/kg; Sigma-Aldrich, St. Louis, MO, USA), after which T10 laminectomy was performed to expose the dura mater. Then, the spine was fixed, and the NYU weight-drop device (New York University, New York, NY, USA) was used to strike the exposed dura mater (the 10-g weight was allowed to fall freely from a height of 2.5 cm above the exposed dura mater) to induce the tail swinging reflex and flaccid paralysis [Basso, Beattie, Bresnahan (BBB) Locomotor Rating Scale score less than 2 points]. After surgery, artificial bladder massage was performed twice a day to encourage urination until the rats resumed spontaneous micturition. All procedures were performed by the same individual. Rats in the sham group were subjected to laminectomy without SCI induction.

Drug treatment
At 1 day after surgery, the rats in the lithium group were injected intraperitoneally with 10 mL of phosphate buffered solution (PBS) containing 85 mg/kg lithium chloride (LiCl; Sigma-Aldrich Co., Gillingham, Dorset, UK) once a day. The sham and SCI groups received 10 mL of PBS.

PC12 cell culture and treatment
PC12 cells (RRID: CVCL_0481; American Type Culture Collection, Manassas, VA, USA) were identified by short tandem repeat (STR). They were cultured in Dulbecco's modified Eagle medium (Gibco, Gaithersburg, MD, USA) containing 5% fetal bovine serum (Gemini Bio-Products, West Sacramento, CA, USA), 10% horse serum (Gemini Bio-Products), and 1% penicillin and streptomycin (Sigma-Aldrich) in a constant-temperature incubator (HASUC, Shanghai, China) set at and at 37°C in a 5% CO_2 atmosphere. The cells were randomly divided into four groups: control, OGD, lithium (OGD + lithium), and all-trans retinoic acid (ATRA) (OGD + lithium + ATRA). For the OGD group, the medium was replaced with glucose-free Dulbecco's modified Eagle medium, and the

cells were incubated in an atmosphere containing 5% CO_2, 0.02% O_2, and 94.98% N_2 at 37°C for 6 hours. The cells were pretreated with LiCl (5 nM) and ATRA [an Nrf2 inhibitor (Wang et al., 2007); 10 μM, Sigma-Aldrich] for 3 hours before OGD.

Motor function evaluation
Six rats in each group were assessed at 1, 3, 5, 7, 14, 21, and 28 days after SCI for functional recovery using the BBB Locomotor Rating Scale (Basso et al., 1995). The BBB score range was 0–21 points. Locomotor ability was scored independently by two assessors (JL and JXL) who were blinded to the grouping but familiar with the scoring criteria. The scores recorded by the two observers were averaged. The rats were subjected to the inclined plate test (using an inclined plane with a rubberized surface on which the greatest angle that the rats could maintain for 5 seconds without sliding was recorded) 30 minutes after BBB scoring. Each of the two observers (JL and JXL) assessed the motor function of each rat twice, and the results were averaged across the two observers.

Tissue processing
At 7 days after surgery, six rats randomly selected from each group were sacrificed under deep anesthesia with 3% pentobarbital sodium. Spinal cord tissue at T10 level was removed, post-fixed in 4% paraformaldehyde, cryoprotected in 30% sucrose, embedded in OCT, and then sectioned using a constant-temperature frozen slicer (Thermo Fisher Scientific, Waltham, MA, USA). Sections (6-μm-thick) from the middle of soma were selected for analysis. Sections preserved at −80°C were used for hematoxylin-eosin (HE) staining, Nissl staining, and immunofluorescence and immunohistochemical analyses. Seven days after surgery, another six rats from each group were subjected to cardiac perfusion, after which the spinal cord tissue at the contusion epicenter was collected and stored at −80°C for later western blotting, enzyme-linked immunosorbent assay (ELISA), and peroxide activity detection.

Histological staining
HE and Nissl staining
Standard HE and Nissl staining of frozen sections were performed to observe the morphology and structure of nerve cells in the spinal cord tissue. For HE staining, sections were submerged in hematoxylin for 5 minutes, washed with water, and then treated with a solution of 1% HCl in ethanol for 30 seconds. Then the sections were stained with eosin for 6 minutes, followed by dehydration with an ethanol gradient (85%, 90%, and 100%). For Nissl staining, sections were submerged in a 1% toluidine blue solution (Sigma-Aldrich) for 15 minutes. Nissl differentiation was then performed for 4–8 seconds until most of the stain was eliminated. Finally, the sections were dehydrated in an ethanol series and cleared with xylene. Image Pro Plus 6 software (Media Cybernetics, Rockville, MD, USA) was used to analyze HE and Nissl staining. The ratio of the area of cavity space to the area of the lesion center was calculated for HE staining, and the number of positively stained cells was calculated for Nissl staining.

Immunohistochemical staining
Immunohistochemical staining was used to detect Caspase-1 and IL-1β expression in spinal cord tissue to evaluate pyroptosis and inflammation, respectively. Frozen sections were fixed in 4°C acetone, inactivated in 3% hydrogen peroxide, incubated with 0.3% Triton X-100 for 20 minutes, and blocked with 10% goat serum for 30 minutes. Then the sections were incubated at 4°C overnight with rat anti-Caspase-1 monoclonal antibody (1:100, BioLegend, San Diego, CA, USA; Cat# 645102, RRID:AB_2068900) and rat anti-IL-1β monoclonal antibody (1:100, Leinco Technologies, Fenton, MO, USA; Cat# I-672, RRID:AB_2830793). Next, the sections were washed with PBS, incubated at room temperature with horseradish peroxidase-conjugated rabbit anti-rat IgG (1:1000, Biorbyt, St. Louis, MO,

USA; Cat# orb21598, RRID:AB_10921028) for 1 hour, and stained with a diaminobenzidine solution (Abcam, Berlin, Germany) for 10 minutes. The number of positive cells was calculated using Image Pro Plus 6 software.

Immunofluorescence staining
Nrf2 and HO-1 in spinal cord tissue and cells were detected by immunofluorescence to evaluate immunopositivity for components of the Nrf2/HO-1 axis. After fixation, infiltration, and sealing, the sections were incubated at 4°C overnight with a rat anti-Nrf2 monoclonal antibody (1:100, Abnova, Taipei, China; Cat# H00004780-M03, RRID:AB_581870) and a rat anti-HO-1 monoclonal antibody (1:1000, Abcam; Cat# 1922-1, RRID:AB_764541). After incubation at room temperature with Alexa Fluor 488 conjugated-rabbit anti-rat IgG (1:50, Imgenex, Bhubaneswar, India; Cat# 20214AF488, RRID:AB_10597709) for 1 hour, the slices were counterstained with 4′,6-diamidino-2-phenylindole (Vector Laboratories, Burlingame, CA, USA) for 10 minutes. A fluorescence microscope (IX71; Olympus, Tokyo, Japan) was used to image the stained cells and tissues. ImageJ software (version 1.8.0; National Institutes of Health, Bethesda, MD, USA) was used to analyze the fluorescence results. The number of positive cells was calculated.

ELISA
The concentrations of IL-6, IL-1β, and tumor necrosis factor-alpha (TNF-α) in spinal cord tissue and cells were detected using an ELISA assay kit (Boster Biological Technology, Wuhan, Hunan Province, China) to evaluate the inflammation. All procedures were carried out in strict accordance with the manufacturer's instructions. A standard curve was generated using a microplate reader (Thermo Scientific, Waltham, MA, USA). Each value represents the mean of triplicate measurements.

Determination of the activity of oxidizing substances
The levels of GSH-Px, SOD, MDA, CAT, T-AOC, and LPO in spinal cord tissue and the levels of GSH-P, SOD, MDA, CAT, T-AOC, and lactate dehydrogenase (LDH) in cells were detected using a biological assay kit (Shanghai Ke Shun, Shanghai, China). A fluorescence probe-DHE (Shanghai BestBio, Shanghai, China) was used to measure the content of reactive oxygen species (ROS). All procedures were performed strictly according to the manufacturer's instructions. ROS production was quantified using a FLUOstar OPTIMA fluorimeter (Thermo Scientific) set to excitation and emission wavelengths of 485 and 520 nm, respectively. The mean fluorescence intensity of ROS was calculated and analyzed using ImageJ, and the results were normalized to the sham group.

Western blot assay
IL-6, IL-1β and TNF-α expression levels were measured to evaluate the inflammatory response in spinal cord tissue and cells. NLRP3, apoptosis-associated speck-like protein containing a CARD (ASC), pro-Caspase-1, Caspase-1, GSDMD, and IL-18 levels were measured to evaluate pyroptosis. Nrf2 and HO-1 levels were measured to assess the Nrf2/HO-1 signaling axis. First, 100 mg of spinal cord tissue was washed with PBS, fully lysed with radioimmunoprecipitation assay buffer (Beyotime, Shanghai, China) containing phenylmethylsulfonyl fluoride for 30 minutes, incubated on ice, and immediately centrifuged at 4°C. The supernatants were then collected, and the protein concentrations was determined using the bicinchoninic acid method (Abdulrahman et al., 2018) with the Pierce™ BCA Protein Assay Kit (Thermo Fisher Scientific). The samples were loaded onto a polyacrylamide gel and electrophoresed. Next, the proteins were transferred to polyvinylidene fluoride membranes and blocked in 5% non-fat milk for 2 hours. Subsequently, the membranes were incubated overnight at 4°C with rat monoclonal primary antibodies against IL-6 (1:1000, Acris Antibodies GmbH, Herford, Germany; Cat# SM1695PX, RRID:AB_1004115), IL-1β (1:100, Miltenyi Biotec, Bergisch

Gladbach, Germany; Cat# 130-125-220, RRID:AB_2889697), TNF-α (1:100, Miltenyi Biotec; Cat# 130-102-386, RRID:AB_2661141), NLRP3 (1:1000, MyBioSource, San Diego, CA, USA; Cat# MBS604215, RRID:AB_10911109), ASC (1:2000, Gabriel Núñez, University of Michigan, Ann Arbor, MI, USA; Cat# GN-ASC, RRID:AB_2750645), pro-Caspase-1 (1:1000, ProSci, San Diego, CA, USA; Cat# 48-495, RRID:AB_1945485), Caspase-1 (1:1000, Acris Antibodies GmbH; Cat# AP06610PU-N, RRID:AB_1611115), GSDMD (1:100, Thermo Fisher Scientific; Cat# A305-736A-M, RRID:AB_2782894), and IL-18 (1:100, DSHB, Iowa City, IA, USA; Cat# CPTC-IL18-2, RRID:AB_1553716), followed by incubation with horseradish peroxidase-conjugated rabbit anti-rat IgG (1:1000, Biorbyt, Cat# orb21564, RRID:AB_10932535) at 20°C for 1 hour, and finally stained with a diaminobenzidine solution. A Bio-Image (Bio-Rad Laboratories, Hercules, CA, USA) gel imaging system was used to collect images. The optical density was measured using ImageJ software. Glyceraldehyde-3-phosphate dehydrogenase (1:1000, LSBio (LifeSpan), Seattle, WA, USA; Cat# LS-C94067-150, RRID:AB_1932766) and β-actin (1:1000, Santa Cruz Biotechnology, Santa Cruz, CA, USA; Cat# sc-47778 HRP, RRID:AB_2714189) were used as internal references.

Flow cytometry

The cells in each group were collected, washed once with PBS, and then centrifuged. The supernatant was discarded, and the cells were washed one more time with PBS. Then the cells were stained with Annexin V, propidium iodide, and fluorescein isothiocyanate isomer (Sigma-Aldrich) in the dark for 30 minutes. Pyroptosis was assessed by flow cytometry (Guava easyCyte™ 8, Millipore, Burlington, VT, USA).

Statistical analysis

All data are expressed as mean ± standard deviation (SD). Statistical analyses and graphs were generated using GraphPad Prism 8 (GraphPad, La Jolla, CA, USA). One-way analysis of variance followed by the least significant difference test was performed to analyze differences among groups. $P < 0.05$ was considered statistically significant.

Results

Lithium alleviates motor dysfunction and pathological damage in rats with SCI

To investigate whether lithium can improve motor function in rats with SCI, we determined BBB scores and performed inclined plate tests at 1, 3, 5, 7, 14, and 28 days after surgery in SCI rats. As shown in **Figure 1**, while the rats in the sham group had no dyskinesia, those in the other two groups had severe dyskinesia that gradually resolved over the duration of the experiment. In addition, the BBB scores in the lithium group were significantly higher than those in the SCI group from the 5th day after surgery ($P < 0.05$; **Figure 1A**). Similar results were obtained with the inclined plated test (**Figure 1B**). Taken together, these results show that lithium can improve mobility in SCI rats.

HE staining of tissue samples from the sham group showed intact structures and clear boundaries between gray and white matter, no neuronal apoptosis in spinal cord tissue, normal nerve cell morphology in the spinal cord, and clearly visible nuclei. In the SCI group, the boundaries between gray and white matter were obscured, and broad areas of hemorrhage were obvious. In addition, the nerve cells in spinal cord were constricted, and their numbers were greatly reduced. The level of neuronal damage in the lithium group was milder than that in the SCI group, but more severe than that in the sham group (**Figure 1C**). The ratio of the area of cavity space to the area of the lesion center in the lithium group was lower than that in the SCI group ($P < 0.05$; **Figure 1D**).

In the sham group, Nissl staining showed that the spinal cord was filled with intact and granular-like neurons. In the SCI group, however, there was a markedly lower number of neurons in the injured tissue area, and the neurons had irregular morphology, indicating neuronal loss through necrosis and apoptosis after SCI (**Figure 1E**). The number of Nissl bodies was significantly greater in the lithium group than in the SCI group at 7 days after surgery ($P < 0.05$; **Figure 1F**).
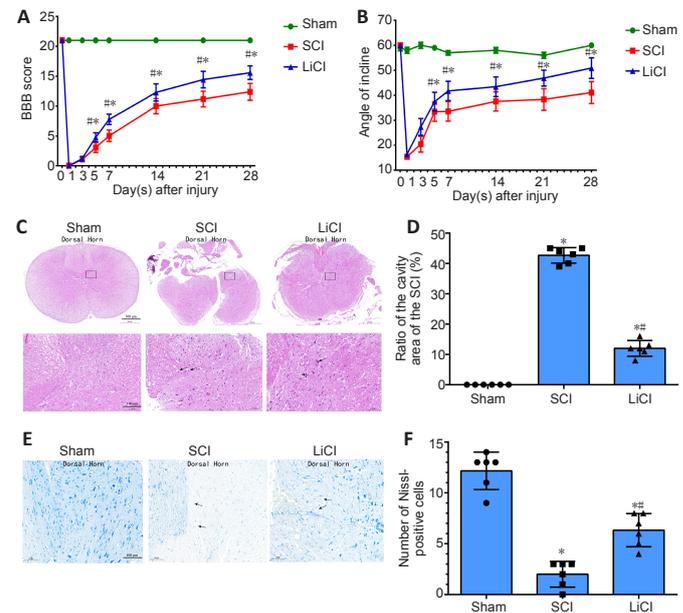

Figure 1 │ Lithium promotes recovery of motor function and tissue repair in rats with spinal cord injury (SCI).
Sham group: No spinal cord injury or treatment; SCI group: spinal cord injury only; LiCl group: lithium treatment after spinal cord injury. (A) Basso, Beattie, Breshman (BBB) Locomotor Rating Scale scores. (B) Inclined plane test. (C) Representative hematoxylin-eosin staining of spinal cord sections 7 days after surgery. The neuronal damage in the LiCl group was more severe than that in the sham group, but less severe than that in the SCI group. Black arrows indicate ruptured cells. Scale bars: 500 μm (upper), 100 μm (lower). (D) Quantification of the ratio of the area of cavity space to the area of the lesion center 7 days after surgery. (E) Representative images of Nissl staining of spinal cord sections 7 days after surgery. The number of neurons in the injured area was lower in the LiCl group than in the sham group, but higher than in the SCI group. Black arrows indicate neurons with irregular morphology. Scale bars: 100 μm. (F) The number of Nissl-positive cells per 0.05 mm² 7 days after surgery. Data are shown as mean ± SD ($n = 6$). *$P < 0.05$, vs. sham group; #$P < 0.05$, vs. SCI group (one-way analysis of variance followed by the least significant difference test). LiCl: Lithium chloride; SCI: spinal cord injury.

Lithium alleviates spinal cord inflammation in rats after SCI

The levels of IL-6, IL-1β, and TNF-α expression in rat spinal cord tissue after SCI were detected by enzyme-linked immunosorbent assay to evaluate inflammation (**Figure 2A–C**). TNF-α was expressed at significantly higher levels in the SCI group than in the sham group. Lithium administration significantly reduced TNF-α expression compared with the SCI group ($P < 0.05$). The levels of IL-6 and IL-1β exhibited similar trends, as they were significantly lower in the lithium group compared with the SCI group (**Figure 2A–C**). As shown in **Figure 2D**, immunohistochemical staining showed that the number of IL-1β-positive cells in the SCI group was significantly higher than that in the sham group ($P < 0.05$). After lithium treatment, the positive staining in the spinal cord tissue was significantly weaker than that in the SCI group ($P < 0.05$; **Figure 2E**). Consistent with this, western blotting revealed that TNF-α, IL-6, and IL-1β protein expression was significantly higher in the spinal cord tissue of SCI rats than in the sham group ($P < 0.05$; **Figure 2F** and **G**). Treatment with lithium reduced the expression levels of these inflammatory factors compared with the SCI group ($P < 0.05$). These results strongly suggest that lithium treatment mitigates SCI by activating anti-inflammatory pathways.
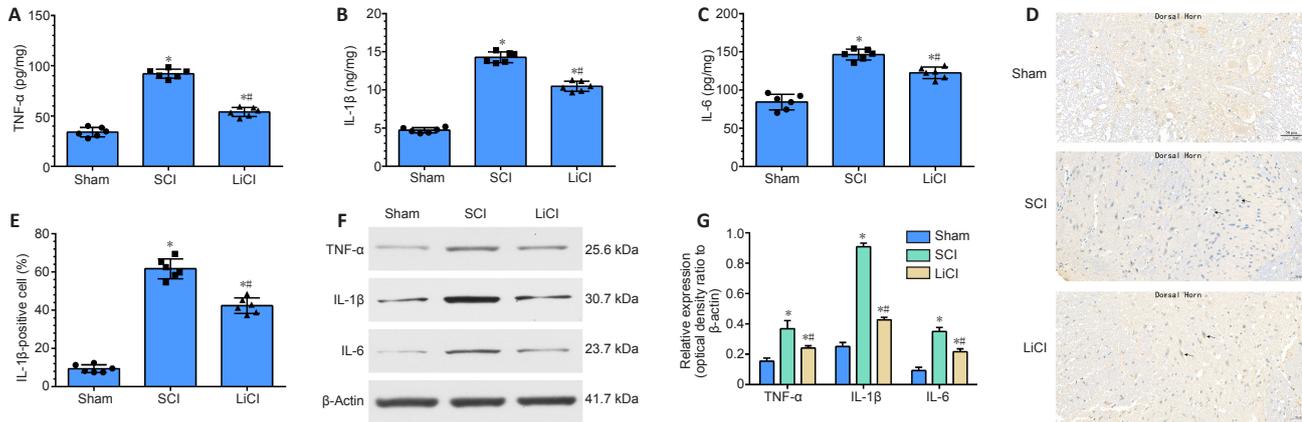
Figure 2 | Lithium suppresses activation of inflammatory cytokines in the spinal cord of rats with SCI.
Sham group: No spinal cord injury or treatment; SCI group: spinal cord injury only; LiCl group: lithium treatment after spinal cord injury. (A–C) TNF-α (A), IL-1β (B), and IL-6 (C) expression in the spinal cord were detected by enzyme-linked immunosorbent assay. (D) Representative immunohistochemical staining for IL-1β 7 days after surgery. The number of IL-1β-positive cells was higher in the LiCl group than in the sham group, but lower than in the SCI group. Black arrows indicate IL-1β-positive cells. Scale bars: 50 μm. (E) Quantification of IL-1β-positive cells 7 days after surgery. (F, G) TNF-α, IL-1β, and IL-6 expression. Data are shown as mean ± SD (n = 6). *P < 0.05, vs. sham group; #P < 0.05, vs. SCI group (one-way analysis of variance followed by the least significant difference test). IL-1β: Interleukin-1β; IL-6: interleukin-6; LiCl: lithium chloride; SCI: spinal cord injury; TNF-α: tumor necrosis factor-alpha.

Lithium suppresses oxidative damage in the spinal cord of rats with SCI

CAT, GSH-Px, LPO, SOD, MDA, and T-AOC are markers of oxidative changes that occur with injury. In the SCI group, CAT, GSH-Px, SOD, and T-AOC levels were decreased, and LPO and MDA levels were significantly increased, compared with the sham group (P < 0.05). In the lithium group, LPO and MDA levels were decreased, and CAT, GSH-Px, SOD, and T-AOC levels were significantly increased compared with the SCI group (all P < 0.05; **Figure 3A–F**). Additionally, there was a marked increase in DHE fluorescence intensity (indicating ROS) after SCI. Lithium treatment resulted in significantly decreased mean ROS fluorescence intensity compared with the sham group (P < 0.05; **Figure 3G**). These results indicate that, in addition to promoting the expression of anti-inflammatory factors, lithium also protects the spinal cord against injury through an anti-oxidant mechanism.
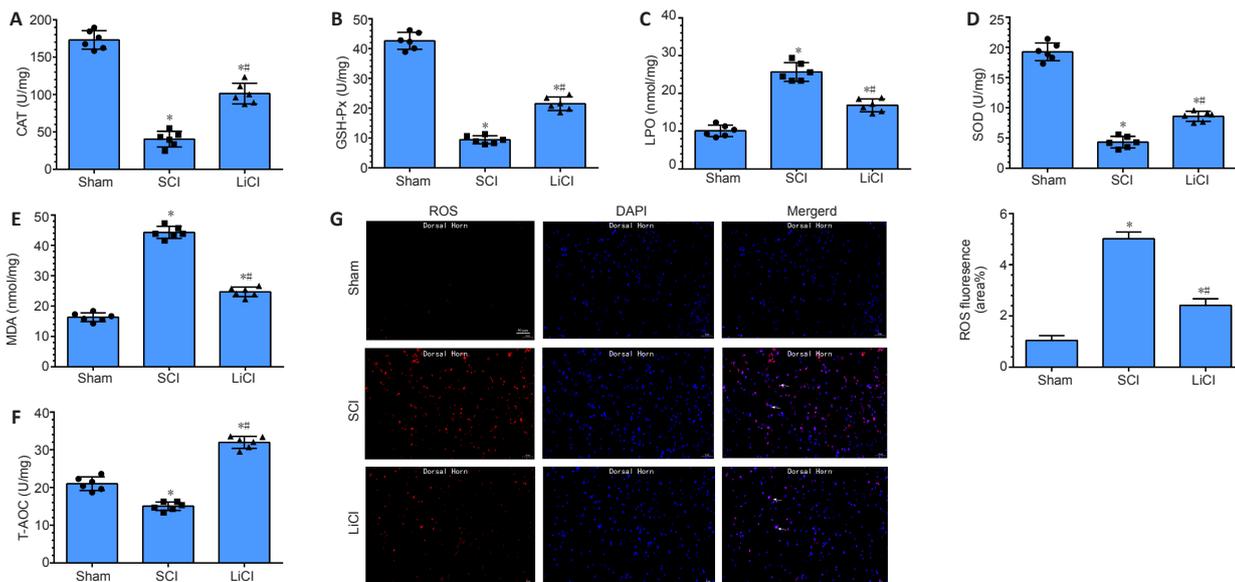

Figure 3 | Lithium reduces oxidative damage in the spinal cord of rats with SCI.
Sham group: No spinal cord injury or treatment; SCI group: spinal cord injury only; LiCl group: lithium treatment after spinal cord injury. (A–F) Effect of lithium on CAT (A), GSH-Px (B), LPO (C), SOD (D), MDA (E), and T-AOC (F) levels in the spinal cord. (G) Representative dihydroethidium (DHE) fluorescence staining and histogram images of reactive oxygen species in injured spinal cord. The fluorescence intensity was higher in the LiCl group than in the sham group, but lower than in the SCI group. White arrows indicate cells with ROS-positive (red) cell nuclei (blue). Scale bars: 50 μm. Data are shown as mean ± SD (n = 6). *P < 0.05, vs. sham group; #P < 0.05, vs. SCI group (one-way analysis of variance followed by the least significant difference test). CAT: Catalase; DAPI: 4',6-diamidino-2-phenylindole; GSH-Px: glutathione peroxidase; LiCl: lithium chloride; LPO: lipid peroxide; MDA: malondialdehyde; ROS: reactive oxygen species; SCI: spinal cord injury; SOD: superoxide dismutase; T-AOC: total antioxidant capacity.

Lithium inhibits pyroptosis in the spinal cord of rats with SCI

Pyroptosis plays a special role in the pathogenesis of SCI. Increased Caspase-1 expression and activation are crucial to the progress of pyroptosis after induction of SCI (Dai et al., 2019). Therefore, we performed immunohistochemical staining of spinal cord tissue for Caspase-1 7 days after SCI. Only a small number of Caspase-1-positive cells were observed in the sham group, while more Caspase-1-positive were observed in the SCI group. The number of Caspase-1-positive cells was significantly lower in the lithium group than in the SCI group (P < 0.05; **Figure 4A** and **B**), suggesting that lithium significantly suppressed the activation of Caspase-1 in SCI. Western blotting showed that NLRP3, ASC, Pro-caspase-1, Caspase-1, GSDMD, and IL-18 were expressed at significantly higher levels in the SCI group than in the sham group, while treatment with lithium significantly decreased expression of these proteins (P < 0.05; **Figure 4C** and **D**). Taken together, these results suggest that lithium inhibited pyroptosis after SCI in rats.
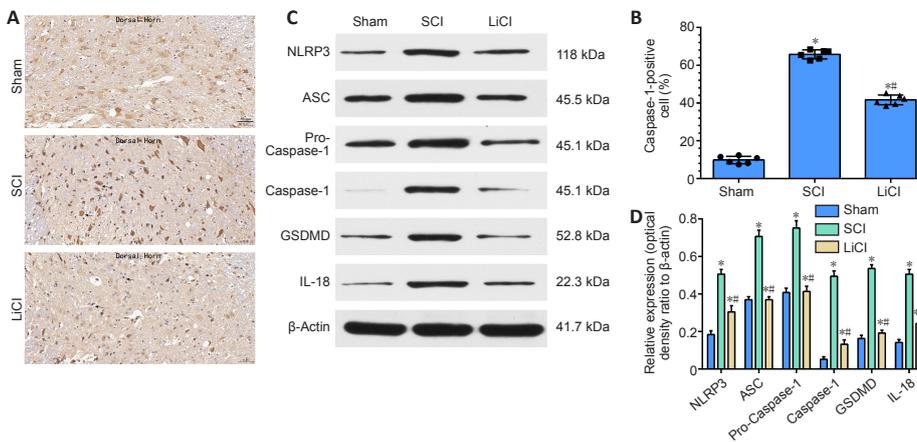
Figure 4 | Lithium inhibits pyroptosis in the spinal cord of rats with SCI.
Sham group: no spinal cord injury or treatment; SCI group: spinal cord injury only; LiCl group: lithium treatment after spinal cord injury. (A) Representative images of immunohistochemistry staining for Caspase-1 7 days after surgery. The number of Caspase-1–positive cells was higher in the LiCl group than in the sham group, but lower than in the SCI group. Black arrows indicate Caspase-1–positive neurons. Scale bars: 50 μm. (B) Quantitation of Caspase-1–positive cells per 1 mm2 7 days after injury. (C) NLRP3, ASC, pro-Caspase-1, Caspase-1, GSDMD, and IL-18 expression in the spinal cord. (D) Quantification of NLRP3, ASC, pro-Caspase-1, Caspase-1, GSDMD, and IL-18 expression in the spinal cord. Data are shown as mean ± SD (n = 6). *$P < 0.05$, *vs.* sham group; #$P < 0.05$, *vs.* SCI group (one-way analysis of variance followed by the least significant difference test). ASC: Apoptosi-associated speck-like protein; GSDMD: gasdermin-d; IL-18: interleukin-18; LiCl: lithium chloride; NLRP3: NOD-like receptors 3; SCI: spinal cord injury.

Lithium promotes Nrf2/HO-1 activation in the spinal cord of rats with SCI

As shown in **Figure 5A** and **B**, compared with the sham group, the protein expression levels of nuclear Nrf2 and cytoplasmic HO-1 were slightly increased in the SCI group. The slight increase in Nrf2 expression may have been associated with the stress response to a severe stimulus. In agreement with the western blot results, immunofluorescence staining showed an increasing trend in Nrf2 and HO-1 expression after SCI. Nuclear Nrf2 and cytoplasmic HO-1 levels were significantly higher in the lithium group than in the SCI group ($P < 0.05$). Additionally, immunofluorescence staining showed that the numbers of nuclear Nrf2- and cytoplasmic HO-1-positive cells were significantly higher in the lithium group than in the SCI group (**Figure 5C**), indicating that treatment with lithium may reduce oxidative stress in injured spinal cord tissue through the Nrf2/HO-1 pathway.
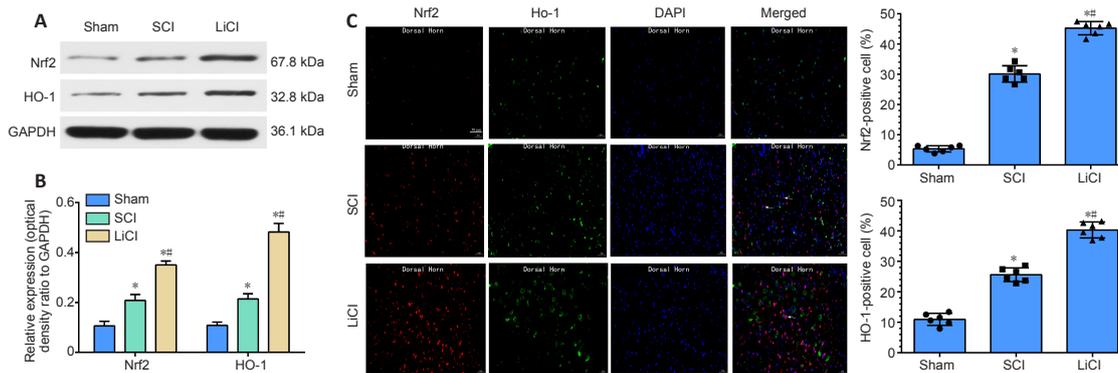

Figure 5 | Lithium up-regulates the Nrf2/HO-1 signaling pathway in the spinal cord of rats with SCI.
Sham group: no spinal cord injury or treatment; SCI group: spinal cord injury only; LiCl group: lithium treatment after spinal cord injury. (A, B) Nrf2 and HO-1 expression in the spinal cord 7 days after surgery. Data are shown as mean ± SD (n= 6). *$P < 0.05$, *vs.* sham group; #$P < 0.05$, *vs.* SCI group (one-way analysis of variance followed by least significant difference test). (C) Representative immunofluorescence images of Nrf2/HO-1 at 7 days after surgery. There were more nuclear Nrf2- and cytoplasmic HO-1-positive cells in the LiCl group than in the SCI group, and in the SCI group than in the sham group. White arrows indicate neurons that were positive for Nrf2 staining (red, Alexa Fluor 647), HO-1 staining (green, Alexa Fluor 488), nuclear staining (blue, DAPI). Scale bars: 50 μm. Data are shown as mean ± SD (n = 6). *$P < 0.05$, *vs.* sham group; #$P < 0.05$, *vs.* SCI group (one-way analysis of variance followed by least significant difference test). DAPI: 4',6-Diamidino-2-phenylindole; HO-1: heme oxygenase-1; LiCl: lithium chloride; Nrf2: nuclear factor E2-related factor 2; SCI: spinal cord injury.

Lithium attenuates inflammatory and oxidative injury in PC12 cells subjected to OGD

To confirm the effects of lithium treatment on inflammation and oxidative stress *in vitro*, PC12 cells were subjected to OGD and treated with lithium. Nrf2 expression is reported to increase after administration of lithium (Castillo-Quan et al., 2016), suggesting that it is a potential target for lithium. Therefore, we specifically investigated the role of Nrf2 inhibition in PC12 cells subjected to OGD and treated with lithium.

IL-1β, IL-6, and TNF-α play an important role in inflammation (Schneider et al., 2019). IL-1β, IL-6, and TNF-α expression levels were significantly increased after the cells were subjected to OGD, and treatment with lithium significantly downregulated their expression compared with the OGD group. This effect was reversed by ATRA, an Nrf2 inhibitor, although inflammatory factor expression did not recover to the levels seen in the OGD group ($P < 0.05$; **Figure 6A–C**).

A number of indicators were evaluated to determine the level of oxidative stress in PC12 cells subjected to OGD. In the OGD group, CAT, GSH-Px, SOD, and T-AOC levels were decreased, and MDA and LDH levels were significantly increased compared with the control group. Compared with the OGD group, cells pretreated with lithium exhibited decreased levels of MDA and LDH but increased levels of GSH-Px, SOD, CAT, and T-AOC. However, there were no significant differences in T-AOC, CAT, or LDH expression levels between the ATRA and LiCl groups ($P < 0.05$; **Figure 6D–I**).

Lithium alleviates pyroptosis and necrosis in PC12 cells subjected to OGD

PI and Annexin V double-staining was used to label pyroptotic cells (**Figure 6J–N**, upper right quadrant) (Miao et al., 2010). The pyroptosis rate in the OGD group was markedly higher than that in the control group. In addition, the lithium and ATRA groups exhibited lower pyroptosis rates than the OGD group. Next, flow cytometric analysis of Annexin V–positive and PI-negative staining was used to identify apoptotic cells (Chi et al., 2020). There was no significant difference in pyroptosis rates among the OGD, LiCl, and ATRA groups (**Figure 6J–N**, upper left quadrant; $P < 0.05$). Taken together, these findings indicate that lithium treatment has a vital neuroprotective effect in protecting cells against OGD-induced pyroptosis.
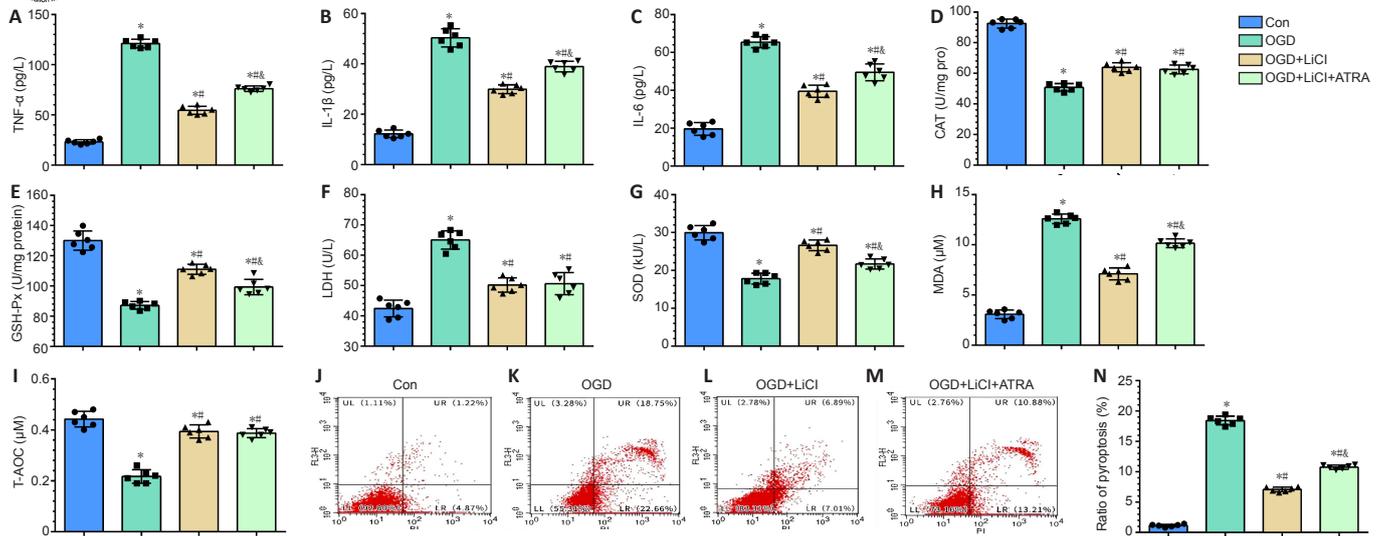
Figure 6 | Lithium attenuates inflammatory, oxidative, and pyroptotic injury in PC12 cells subjected to OGD.
Con group: untreated PC12 cells; OGD group: PC12 cells subjected to OGD; OGD + LiCl group: PC12 cells subjected to OGD and treated with LiCl; OGD + LiCl + ATRA group: PC12 cells subjected to OGD and treated with LiCl and the Nrf2 inhibitor ATRA. (A–I) TNF-α (A), IL-1β (B), IL-6 (C), CAT (D), GSH-Px (E), LDH (F), SOD (G), MDA (H), and T-AOC (I) expression as detected by ELISA. (J–N) Flow cytometry analysis of the percentage of pyroptotic PC12 cells. Data are shown as mean ± SD ($n = 6$). *$P < 0.05$, vs. control group; #$P < 0.05$, vs. OGD group; &$P < 0.05$, vs. OGD + LiCl group (one-way analysis of variance followed by least significant difference test). ATRA: All-trans retinoic acid; CAT: catalase; Con: control; GSH-Px: glutathione peroxidase; IL-1β: interleukin-1β; IL-6: interleukin-6; LiCl: lithium chloride; LPO: lipid peroxide; MDA: malondialdehyde; OGD: oxygen glucose deprivation; SOD: superoxide dismutase; T-AOC: total antioxidant capacity; TNF-α: tumor necrosis factor-alpha.

Western blotting was used to assess the expression levels of some key proteins involved in pyroptosis. NLRP3, ASC, pro-Caspase-1, Caspase-1, GSDMD, and IL-18 expression levels were markedly increased in the OGD group compared with the control group. This effect was largely reversed by lithium. The expression level of all pyroptosis-related proteins, with the exception of pro-Caspase-1, was significantly increased in the ATRA group compared with the lithium group ($P < 0.05$; **Figure 7A** and **B**). Therefore, we concluded that lithium inhibits pyroptosis by downregulating NLRP3, ASC, pro-Caspase-1, Caspase-1, GSDMD, and IL-18 expression.

Lithium protects PC12 cells from OGD-induced damage through the Nrf2/HO-1 pathway

To investigate the possible mechanism by which lithium protects PC12 cells from pyroptosis, we assessed changes in Nrf2 and HO-1 expression levels induced by OGD. Western blotting showed that treatment with lithium greatly increased the levels of Nrf2 and HO-1 compared with the OGD group, and this effect was significantly reversed by treatment with ATRA ($P < 0.05$; **Figure 7C** and **D**). These findings were confirmed by immunofluorescence (**Figure 7E** and **F**).
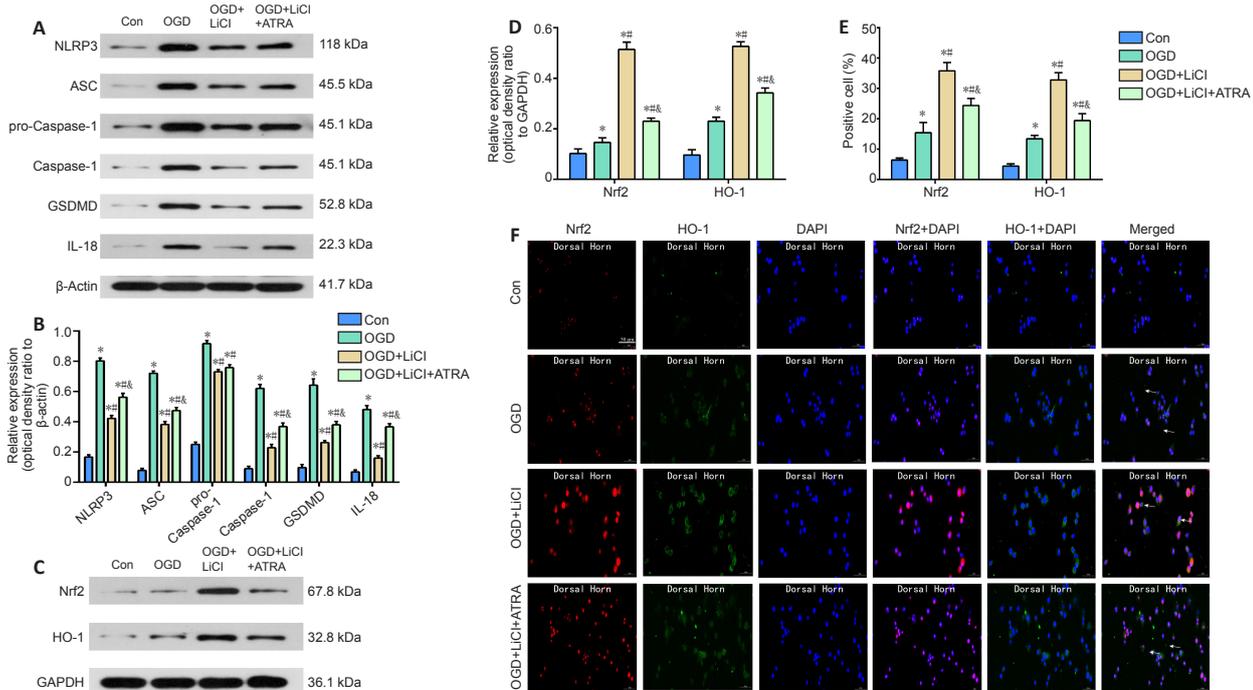

Figure 7 | Lithium attenuates pyroptotic injury by activating the Nrf2/HO-1 signaling pathway in PC12 cells subjected to OGD.
Con group: untreated PC12 cells; OGD group: PC12 cells subjected to OGD; OGD + LiCl group: PC12 cells subjected to OGD and treated with LiCl; OGD + LiCl + ATRA group: PC12 cells subjected to OGD and treated with LiCl treatment and the Nrf2 inhibitor ATRA. (A, B) NLRP3, ASC, pro-Caspase-1, Caspase-1, GSDMD, and IL-18 expression. (C, D) Nrf2 and HO-1 expression. (E) The expression levels of pyroptosis-related proteins were significantly higher in the OGD group than in the Con group, and this effect was largely reversed by treatment with LiCl. The expression levels of these proteins were significantly higher in the ATRA group than in the LiCl group, with the exception of pro-Caspase-1. Nrf2 and HO-1 expression levels were significantly increased by LiCl treatment, and this effect was largely reversed by treatment with the Nrf2 inhibitor ATRA. Data are shown as mean ± SD ($n = 6$). *$P < 0.05$, vs. control group; #$P < 0.05$, vs. OGD group; &$P < 0.05$, vs. OGD + LiCl group (one-way analysis of variance followed by least significant difference test). (F) Representative images of Nrf2 and HO-1 immunofluorescence. White arrows indicate neurons that were positive for Nrf2 staining (red, Alexa Fluor 647), HO-1 staining (green, Alexa Fluor 488), and cell nucleus staining (blue, DAPI). Scale bar: 50 μm. ASC: Apoptosis-associated speck-like protein; ATRA: all-trans retinoic acid; DAPI: 4′,6-diamidino-2-phenylindole; GSDMD: gasdermin-d; HO-1: heme oxygenase-1; IL-18: interleukin-18; LiCl: lithium chloride; NLRP3: NOD-like receptors 3; Nrf2: nuclear factor E2-related factor 2; OGD: oxygen glucose deprivation.

Discussion

In this study, we investigated the therapeutic effects of lithium treatment in a rat model of SCI. Our results indicate that lithium therapy partially improved the motor ability of rats with SCI and alleviated spinal cord inflammation. We found that lithium up-regulated the expression of Nrf2, down-regulated the expression of HO-1, and increased the expression of CAT, GSH-Px, SOD, and T-AOC, thereby inhibiting neuronal pyroptosis. Our results also showed that lithium alleviated inflammation, inhibited oxidative stress, and inhibited neuronal pyroptosis via the Nrf2/HO-1 pathway in rats with SCI. Further research is needed to confirm our results and further clarify the mechanism by which lithium exerts these effects.

Evaluation of neurological function is necessary for assessing recovery after SCI (Gomez et al., 2018). In the current study, behavioral tests revealed that lithium promoted the recovery of hindlimb motor function in rats after acute SCI. The therapeutic effect may be related to lithium-mediated reduction in nerve cell and tissue damage and promotion of neuromotor function recovery. After treatment with lithium, the neuronal structure at the SCI site gradually clarified, and the nuclei were clearly visible. Cavitation of Nissl bodies in the neurons was also reduced in the lithium group compared with the SCI group, and the Nissl bodies appeared to be more structurally complete. These findings suggest that lithium alleviates secondary injury after SCI and promotes recovery of neurological function. Our results are consistent with those from many previous studies (Yick et al., 2004; Zakeri et al., 2014; Liu et al., 2017; Tong et al., 2018; Abdanipour et al., 2019)

It is well known that inflammatory factors such as IL-1β, IL-6, and IL-18 can cause serious damage to the nervous system (Li et al., 2017; Zhao et al., 2017; Huang et al., 2019). These key inflammatory molecules adversely affect the survival of neurons and play different roles in the progression of nerve damage (Sobowale et al., 2016; Wytrykowska et al., 2016). These molecules coordinate with each other, promote each others' expression, cause an inflammatory cascade, and greatly amplify the inflammatory response of pyroptotic cells (Dutta et al., 2012; Toldo et al., 2014; Slaats et al., 2016). The results from the current study indicate that inflammatory death of nerve cells (i.e., pyroptosis) is mediated by NLRP3 inflammasomes in a rat model of SCI, and that lithium treatment can reduce the secretion of inflammatory cytokines, thereby reducing the damage caused by SCI.

Oxidative stress is an important factor in the secondary damage that occurs after SCI, and the degree of oxidative stress is directly related to SCI prognosis (Adriaansen et al., 2016). In the current study, treatment with lithium resulted in a significant reduction in the expression levels of these oxidative stress factors, suggesting that lithium can effectively inhibit the oxidative stress response after SCI. Moreover, excessive ROS production has been shown to trigger activation of NLRP3 inflammasomes (Abais et al., 2015). Inhibition of ROS can prevent activation of Caspase-1 and production of IL-18 and IL-1β. The results from our study suggest that oxidative stress may be an important mechanisms underlying post-SCI pyroptosis.

Pyroptosis involving Caspase-1 is considered part of the classical inflammasome pathway, whereas pyroptosis involving Caspases-4, -5, or -11 is considered to be part of the non-classical inflammasome pathway (Barrington et al., 2017). In the current study, we found that Caspase-1 expression was markedly decreased in the lithium group compared with the SCI. Therefore, we believe that the classical inflammasome pathway mediated by Caspase-1, which can be effectively targeted and inhibited by lithium agents, is likely the main

mechanism involved in secondary damage following SCI, rather than the non-classical inflammatory pathway. A past study reported that celastrol inhibits microglial pyroptosis and attenuates inflammation in a rat model of acute SCI (Dai et al., 2019). Taken together with our results, this shows that pyroptosis plays an important role in acute SCI and can be targeted with lithium, which is a more commonly used and more effective drug.

To determine the molecular mechanisms underlying lithium's anti-inflammatory, anti-oxidant, and anti-pyroptotic activities, we assessed the expression levels of components of the Nrf2/HO-1 signaling pathway. Because the complexities of the *in vivo* model would have made it difficult to investigate this in rats, we designed *in vitro* experiments to explore these questions. Our findings showed that treatment with lithium up-regulated the expression of Nrf2 and various anti-oxidant enzymes and down-regulated the expression of various detoxification enzymes, thereby restoring cellular redox balance and exerting endogenous cytoprotective effects. Treating cells with ATRA reversed these effects, indirectly confirming these findings.

The inflammatory response primarily involves neutrophil infiltration and the release of inflammatory factors, and is a key step in secondary SCI (Orr and Gensel, 2018). This study shows that lithium can activate the Nrf2/HO-1 pathway to reduce tissue inflammation. Treating PC12 cells subjected to OGD with an Nrf2 inhibitor decreased inflammation, oxidative stress, and pyroptosis. Moreover, we found that the inflammatory response that occurs after SCI is activated by the NLRP3 inflammasome, which then activates Caspase-1 in the classical pyroptosis pathway. At the same time, excessive ROS generated by oxidative stress after tissue injury can also trigger activation of the NLRP3 inflammasome. Therefore, we speculate that the Nrf2/HO-1 pathway promotes inflammatory cell death by regulating oxidative stress factors *in vivo*. Hou et al. (2018) found that activation of the NLRP3 inflammatory complex plays an important role in the inflammatory process after cerebral ischemia/reperfusion injury. Nrf2 inhibits activation of the NLRP3 inflammatory complex by regulating the thioredoxin/thioredoxin binding protein complex, thus playing a role in alleviating ischemia/reperfusion injury and protecting nerves. Taken together with the results from our study, this suggests that the Nrf2/HO-1 pathway plays a role in various aspects of repair of central nervous system injury. To our knowledge, our study is the first to report that lithium exerts anti-inflammatory, anti-oxidant, and anti-pyroptotic effects through the Nrf2/HO-1 pathway to promote recovery after SCI.

In this study, we did not detect any side effects of lithium treatment in rats. This is consistent with a clinical trial that confirmed the safety of lithium treatment in patients with SCI (Wong et al., 2011). Although older studies have noted potential lithium-induced kidney damage (Vestergaard and Amdisen, 1981; Miller et al., 1985), more recent studies have drawn the opposite conclusion, demonstrating that short-term low-dose lithium may ameliorate kidney and podocyte injury (Wang et al., 2009b; Xu et al., 2014b). Whether lithium negatively affects kidney function remains controversial (Gong et al., 2016).

There were some limitations to this study. In this study, we found that the NLRP3 inflammasome is the main mediator of pyroptosis after SCI. However, some studies have shown that neuronal cells in the spinal cord primarily contain NLRP1 inflammasomes (de Rivero Vaccari et al., 2008). NLRP1 can also mediate neuronal pyroptosis after SCI, but only a few studies have explored this topic, and further research is needed (Kaushal et al., 2015). In addition, the timeline of pyroptosis after SCI has not been studied in detail. One previous study reported that pyroptosis peaks the third day

after SCI (Zheng et al., 2019), while another study pointed to the seventh day after SCI as the most important period for pyroptosis (Dai et al., 2019). However, no study (including our study) has explored changes in pyroptosis over time after SCI. In addition, our study lacked the *in vivo* experiments needed to further verify the relationship between lithium treatment and the Nrf2/HO-1 signaling pathway in rats with SCI. These questions should be the focus of future research.

In summary, our results indicate that pyroptosis is an inflammatory form of programmed cell death, as well as nerve cell death, that occurs in tissues after SCI *in vivo* and in cells after OGD *in vitro*. Lithium treatment can inhibit activation of the NLRP3 inflammasome by inhibiting the oxidative stress response after SCI, reducing spinal cord tissue and inhibiting inflammation and neuronal pyroptosis. Furthermore, the Nrf2/HO-1 signaling pathway, which is a classic regulator of oxidative stress, can also regulate inflammation and pyroptosis after SCI. Further research is needed to identify other possible mechanisms underlying the effect of lithium on SCI.

References

Abais JM, Xia M, Zhang Y, Boini KM, Li PL (2015) Redox regulation of NLRP3 inflammasomes: ROS as trigger or effector? Antioxid Redox Signal 22:1111-1129.

Abdanipour A, Moradi F, Fakheri F, Ghorbanlou M, Nejatbakhsh R (2019) The effect of lithium chloride on BDNF, NT3, and their receptor mRNA levels in the spinal contusion rat models. Neurol Res 41:577-583.

Abdulrahman BA, Abdelaziz DH, Schatzl HM (2018) Autophagy regulates exosomal release of prions in neuronal cells. J Biol Chem 293:8956-8968.

Adriaansen JJ, Ruijs LE, van Koppenhagen CF, van Asbeck FW, Snoek GJ, van Kuppevelt D, Visser-Meily JM, Post MW (2016) Secondary health conditions and quality of life in persons living with spinal cord injury for at least ten years. J Rehabil Med 48:853-860.

Ahuja CS, Nori S, Tetreault L, Wilson J, Kwon B, Harrop J, Choi D, Fehlings MG (2017) Traumatic spinal cord injury-repair and regeneration. Neurosurgery 80:S9-22.

Allen AR (1911) Surgery of experimental lesion of spinal cord equivalent to crush injury of fracture dislocation of spinal column: a preliminary report. J Am Med Assoc LVII:878-880.

Anjum A, Yazid MD, Fauzi Daud M, Idris J, Ng AMH, Selvi Naicker A, Ismail OHR, Athi Kumar RK, Lokanathan Y (2020) Spinal cord injury: pathophysiology, multimolecular interactions, and underlying recovery mechanisms. Int J Mol Sci 21:7533.

Assinck P, Duncan GJ, Hilton BJ, Plemel JR, Tetzlaff W (2017) Cell transplantation therapy for spinal cord injury. Nat Neurosci 20:637-647.

Barrington J, Lemarchand E, Allan SM (2017) A brain in flame; do inflammasomes and pyroptosis influence stroke pathology? Brain Pathol 27:205-212.

Basso DM, Beattie MS, Bresnahan JC (1995) A sensitive and reliable locomotor rating scale for open field testing in rats. J Neurotrauma 12:1-21.

Brotfain E, Gruenbaum SE, Boyko M, Kutz R, Zlotnik A, Klein M (2016) Neuroprotection by estrogen and progesterone in traumatic brain injury and spinal cord injury. Curr Neuropharmacol 14:641-653.

Broz P, Dixit VM (2016) Inflammasomes: mechanism of assembly, regulation and signalling. Nat Rev Immunol 16:407-420.

Castillo-Quan JI, Li L, Kinghorn KJ, Ivanov DK, Tain LS, Slack C, Kerr F, Nespital T, Thornton J, Hardy J, Bjedov I, Partridge L (2016) Lithium Promotes Longevity through GSK3/NRF2-Dependent Hormesis. Cell Rep 15:638-650.

Chi Y, Peng B, Lu J (2020) Effect of ovarian storage time at 4 degrees C on cumulus cell apoptosis in porcine antral follicles. Anim Sci J 91:e13465.

Dai W, Wang X, Teng H, Li C, Wang B, Wang J (2019) Celastrol inhibits microglial pyroptosis and attenuates inflammatory reaction in acute spinal cord injury rats. Int Immunopharmacol 66:215-223.

de Rivero Vaccari JP, Dietrich WD, Keane RW (2014) Activation and regulation of cellular inflammasomes: gaps in our knowledge for central nervous system injury. J Cereb Blood Flow Metab 34:369-375.

de Rivero Vaccari JP, Lotocki G, Marcillo AE, Dietrich WD, Keane RW (2008) A molecular platform in neurons regulates inflammation after spinal cord injury. J Neurosci 28:3404-3414.

Dixon KJ (2017) Pathophysiology of traumatic brain injury. Phys Med Rehabil Clin N Am 28:215-225.

Dutta P, Courties G, Wei Y, Leuschner F, Gorbatov R, Robbins CS, Iwamoto Y, Thompson B, Carlson AL, Heidt T, Majmudar MD, Lasitschka F, Etzrodt M, Waterman P, Waring MT, Chicoine AT, van der Laan AM, Niessen HW, Piek JJ, Rubin BB, et al. (2012) Myocardial infarction accelerates atherosclerosis. Nature 487:325-329.

Dwivedi S, Rajasekar N, Hanif K, Nath C, Shukla R (2016) Sulforaphane ameliorates okadaic acid-induced memory impairment in rats by activating the Nrf2/HO-1 antioxidant pathway. Mol Neurobiol 53:5310-5323.

Gazdic M, Volarevic V, Harrell CR, Fellabaum C, Jovicic N, Arsenijevic N, Stojkovic M (2018) Stem cells therapy for spinal cord injury. Int J Mol Sci 19:1039.

Gökce EC, Kahveci R, Gökce A, Cemil B, Aksoy N, Sargon MF, Kısa Ü, Erdoğan B, Güvenç Y, Alagöz F, Kahveci O (2016) Neuroprotective effects of thymoquinone against spinal cord ischemia-reperfusion injury by attenuation of inflammation, oxidative stress, and apoptosis. J Neurosurg Spine 24:949-959.

Gomez RM, Ghotme K, Nino JJ, Quiroz-Padilla M, Vargas D, Dominguez AR, Barreto GE, Sanchez MY (2018) Combined strategy for a reliable evaluation of spinal cord injury using an in vivo model. Cent Nerv Syst Agents Med Chem 18:49-57.

Gong R, Wang P, Dworkin L (2016) What we need to know about the effect of lithium on the kidney. Am J Physiol Renal Physiol 311:F1168-f1171.

Gu XK, Li XR, Lu ML, Xu H (2020) Lithium promotes proliferation and suppresses migration of Schwann cells. Neural Regen Res 15:1955-1961.

Guttuso T Jr (2019) High lithium levels in tobacco may account for reduced incidences of both Parkinson's disease and melanoma in smokers through enhanced β-catenin-mediated activity. Med Hypotheses 131:109302.

Haupt M, Bähr M, Doeppner TR (2021) Lithium beyond psychiatric indications: the reincarnation of a new old drug. Neural Regen Res 16:2383-2387.

Huang XQ, Liao XQ, Shi CL, Zhang XL (2019) Methylprednisolone inhibits inflammation mediated by activated microglia after spinal cord injury in rat models. Zhongguo Zuzhi Gongcheng Yanjiu 23:3050-3055.

Hou Y, Wang Y, He Q, Li L, Xie H, Zhao Y, Zhao J (2018) Nrf2 inhibits NLRP3 inflammasome activation through regulating Trx1/TXNIP complex in cerebral ischemia reperfusion injury. Behav Brain Res 336:32-39.

Jalali HK, Salamatzadeh A, Jalali AK, Kashani HH, Asbchin SA, Issazadeh K (2016) Antagonistic activity of nocardia brasiliensis PTCC 1422 against isolated enterobacteriaceae from urinary tract infections. Probiotics Antimicrob Proteins 8:41-45.

Ji Q, Gao J, Zheng Y, Liu X, Zhou Q, Shi C, Yao M, Chen X (2017) Inhibition of microRNA-153 protects neurons against ischemia/reperfusion injury in an oxygen-glucose deprivation and reoxygenation cellular model by regulating Nrf2/HO-1 signaling. J Biochem Mol Toxicol 31.

Kalayci M, Coskun O, Cagavi F, Kanter M, Armutcu F, Gul S, Acikgoz B (2005) Neuroprotective effects of ebselen on experimental spinal cord injury in rats. Neurochem Res 30:403-410.

Kaushal V, Dye R, Pakavathkumar P, Foveau B, Flores J, Hyman B, Ghetti B, Koller BH, LeBlanc AC (2015) Neuronal NLRP1 inflammasome activation of Caspase-1 coordinately regulates inflammatory interleukin-1-beta production and axonal degeneration-associated Caspase-6 activation. Cell Death Differ 22:1676-1686.

Kuang S, Zheng J, Yang H, Li S, Duan S, Shen Y, Ji C, Gan J, Xu XW, Li J (2017) Structure insight of GSDMD reveals the basis of GSDMD autoinhibition in cell pyroptosis. Proc Natl Acad Sci U S A 114:10642-10647.

Li XQ, Wang J, Fang B, Tan WF, Ma H (2014a) Intrathecal antagonism of microglial TLR4 reduces inflammatory damage to blood-spinal cord barrier following ischemia/reperfusion injury in rats. Mol Brain 7:28.

Li XQ, Lv HW, Tan WF, Fang B, Wang H, Ma H (2014b) Role of the TLR4 pathway in blood-spinal cord barrier dysfunction during the bimodal stage after ischemia/reperfusion injury in rats. J Neuroinflammation 11:62.

Li Y, Xu L, Zeng K, Xu Z, Suo D, Peng L, Ren T, Sun Z, Yang W, Jin X, Yang L (2017) Propane-2-sulfonic acid octadec-9-enyl-amide, a novel PPARα/γ dual agonist, protects against ischemia-induced brain damage in mice by inhibiting inflammatory responses. Brain Behav Immun 66:289-301.

Liu P, Zhang Z, Wang Q, Guo R, Mei W (2017) Lithium chloride facilitates autophagy following spinal cord injury via ERK-dependent pathway. Neurotox Res 32:535-543.

Liu X, Zhang Z, Ruan J, Pan Y, Magupalli VG, Wu H, Lieberman J (2016) Inflammasome-activated gasdermin D causes pyroptosis by forming membrane pores. Nature 535:153-158.

Ma Q (2013) Role of nrf2 in oxidative stress and toxicity. Annu Rev Pharmacol Toxicol 53:401-426.

Martinon F, Burns K, Tschopp J (2002) The inflammasome: a molecular platform triggering activation of inflammatory caspases and processing of proIL-beta. Mol Cell 10:417-426.

Martinon F, Mayor A, Tschopp J (2009) The inflammasomes: guardians of the body. Annu Rev Immunol 27:229-265.

Medzhitov R (2008) Origin and physiological roles of inflammation. Nature 454:428-435.

Miao EA, Leaf IA, Treuting PM, Mao DP, Dors M, Sarkar A, Warren SE, Wewers MD, Aderem A (2010) Caspase-1-induced pyroptosis is an innate immune effector mechanism against intracellular bacteria. Nat Immunol 11:1136-1142.

Miller AL, Bowden CL, Plewes J (1985) Lithium and impairment of renal concentrating ability. J Affect Disord 9:115-119.

Mortezaee K, Khanlarkhani N, Beyer C, Zendedel A (2018) Inflammasome: Its role in traumatic brain and spinal cord injury. J Cell Physiol 233:5160-5169.

Orr MB, Gensel JC (2018) Spinal cord injury scarring and inflammation: therapies targeting glial and inflammatory responses. Neurotherapeutics 15:541-553.

Pabon M, Tamboli C, Tamboli S, Acosta S, De La Pena I, Sanberg PR, Tajiri N, Kaneko Y, Borlongan CV (2014) Estrogen replacement therapy for stroke. Cell Med 6:111-122.

Pasquali L, Longone P, Isidoro C, Ruggieri S, Paparelli A, Fornai F (2009) Autophagy, lithium, and amyotrophic lateral sclerosis. Muscle Nerve 40:173-194.

Rowe MK, Chuang DM (2004) Lithium neuroprotection: molecular mechanisms and clinical implications. Expert Rev Mol Med 6:1-18.

Rybakowski JK, Suwalska A, Hajek T (2018) Clinical perspectives of lithium's neuroprotective effect. Pharmacopsychiatry 51:194-199.

Schneider L, Reichert E, Faulkner J, Reichert B, Sonnen J, Hawryluk GWJ (2019) CNS inflammation and neurodegeneration: sequelae of peripheral inoculation with spinal cord tissue in rat. J Neurosurg 132:933-944.

Serafini G, Giordano G, Romano S, Raja M, Girardi P, Amore M, Pompili M (2016) Huntington's disease and suicidal behavior: The importance of lithium treatment. Clin Neurol Neurosurg 145:108-109.

Sircar R (2019) Estrogen modulates ethanol-induced memory deficit in postpubertal adolescent rats. Alcohol Clin Exp Res 43:61-68.

Slaats J, Ten Oever J, van de Veerdonk FL, Netea MG (2016) IL-1β/IL-6/CRP and IL-18/ferritin: distinct inflammatory programs in infections. PLoS Pathog 12:e1005973.

Smith PD, Puskas F, Meng X, Lee JH, Cleveland JC, Jr., Weyant MJ, Fullerton DA, Reece TB (2012) The evolution of chemokine release supports a bimodal mechanism of spinal cord ischemia and reperfusion injury. Circulation 126:S110-117.

Sobowale OA, Parry-Jones AR, Smith CJ, Tyrrell PJ, Rothwell NJ, Allan SM (2016) Interleukin-1 in stroke: from bench to bedside. Stroke 47:2160-2167.

Toldo S, Mezzaroma E, O'Brien L, Marchetti C, Seropian IM, Voelkel NF, Van Tassell BW, Dinarello CA, Abbate A (2014) Interleukin-18 mediates interleukin-1-induced cardiac dysfunction. Am J Physiol Heart Circ Physiol 306:H1025-1031.

Tong M, He Z, Lin X, Zhou Y, Wang Q, Zheng Z, Chen J, Xu H, Tian N (2018) Lithium chloride contributes to blood-spinal cord barrier integrity and functional recovery from spinal cord injury by stimulating autophagic flux. Biochem Biophys Res Commun 495:2525-2531.

Tsuchiya K (2020) Inflammasome-associated cell death: pyroptosis, apoptosis, and physiological implications. Microbiol Immunol 64:252-269.

Vestergaard P, Amdisen A (1981) Lithium treatment and kidney function. A follow-up study of 237 patients in long-term treatment. Acta Psychiatr Scand 63:333-345.

Wang L, Li W, Kang Z, Liu Y, Deng X, Tao H, Xu W, Li R, Sun X, Zhang JH (2009a) Hyperbaric oxygen preconditioning attenuates early apoptosis after spinal cord ischemia in rats. J Neurotrauma 26:55-66.

Wang XJ, Hayes JD, Henderson CJ, Wolf CR (2007) Identification of retinoic acid as an inhibitor of transcription factor Nrf2 through activation of retinoic acid receptor alpha. Proc Natl Acad Sci U S A 104:19589-19594.

Wang Y, Huang WC, Wang CY, Tsai CC, Chen CL, Chang YT, Kai JI, Lin CF (2009b) Inhibiting glycogen synthase kinase-3 reduces endotoxaemic acute renal failure by down-regulating inflammation and renal cell apoptosis. Br J Pharmacol 157:1004-1013.

Wong YW, Tam S, So KF, Chen JY, Cheng WS, Luk KD, Tang SW, Young W (2011) A three-month, open-label, single-arm trial evaluating the safety and pharmacokinetics of oral lithium in patients with chronic spinal cord injury. Spinal Cord 49:94-98.

Wu XY, Li KT, Yang HX, Yang B, Lu X, Zhao LD, Fei YY, Chen H, Wang L, Li J, Peng LY, Zheng WJ, Hou Y, Jiang Y, Shi Q, Zhang W, Zhang FC, Zhang JM, Huang B, He W, et al. (2020) Complement C1q synergizes with PTX3 in promoting NLRP3 inflammasome over-activation and pyroptosis in rheumatoid arthritis. J Autoimmun 106:102336.

Wytrykowska A, Prosba-Mackiewicz M, Nyka WM (2016) IL-1β, TNF-α, and IL-6 levels in gingival fluid and serum of patients with ischemic stroke. J Oral Sci 58:509-513.

Xiang J, Cao K, Dong YT, Xu Y, Li Y, Song H, Zeng XX, Ran LY, Hong W, Guan ZZ (2020) Lithium chloride reduced the level of oxidative stress in brains and serums of APP/PS1 double transgenic mice via the regulation of GSK3β/Nrf2/HO-1 pathway. Int J Neurosci 130:564-573.

Xu J, Huang G, Zhang K, Sun J, Xu T, Li R, Tao H, Xu W (2014a) Nrf2 activation in astrocytes contributes to spinal cord ischemic tolerance induced by hyperbaric oxygen preconditioning. J Neurotrauma 31:1343-1353.

Xu W, Ge Y, Liu Z, Gong R (2014b) Glycogen synthase kinase 3β dictates podocyte motility and focal adhesion turnover by modulating paxillin activity: implications for the protective effect of low-dose lithium in podocytopathy. Am J Pathol 184:2742-2756.

Xue F, Shu R, Xie Y (2015) The expression of NLRP3, NLRP1 and AIM2 in the gingival tissue of periodontitis patients: RT-PCR study and immunohistochemistry. Arch Oral Biol 60:948-958.

Yang ML, Li JJ, So KF, Chen JY, Cheng WS, Wu J, Wang ZM, Gao F, Young W (2012) Efficacy and safety of lithium carbonate treatment of chronic spinal cord injuries: a double-blind, randomized, placebo-controlled clinical trial. Spinal Cord 50:141-146.

Yick LW, So KF, Cheung PT, Wu WT (2004) Lithium chloride reinforces the regeneration-promoting effect of chondroitinase ABC on rubrospinal neurons after spinal cord injury. J Neurotrauma 21:932-943.

Yuksel Y, Guven M, Kaymaz B, Sehitoglu MH, Aras AB, Akman T, Tosun M, Cosar M (2016) Effects of aloe vera on spinal cord ischemia-reperfusion injury of rats. J Invest Surg 29:389-398.

Zakeri M, Afshari K, Gharedaghi MH, Shahsiah R, Rahimian R, Maleki F, Dehpour AR, Javidan AN (2014) Lithium protects against spinal cord injury in rats: role of nitric oxide. J Neurol Surg A Cent Eur Neurosurg 75:427-433.

Zhai X, Chen X, Shi J, Shi D, Ye Z, Liu W, Li M, Wang Q, Kang Z, Bi H, Sun X (2013) Lactulose ameliorates cerebral ischemia-reperfusion injury in rats by inducing hydrogen by activating Nrf2 expression. Free Radic Biol Med 65:731-741.

Zhao GC, Yuan YL, Chai FR, Ji FJ (2017) Effect of Melilotus officinalis extract on the apoptosis of brain tissues by altering cerebral thrombosis and inflammatory mediators in acute cerebral ischemia. Biomed Pharmacother 89:1346-1352.

Zhaolin Z, Guohua L, Shiyuan W, Zuo W (2019) Role of pyroptosis in cardiovascular disease. Cell Prolif 52:e12563.

Zheng G, Zhan Y, Wang H, Luo Z, Zheng F, Zhou Y, Wu Y, Wang S, Wu Y, Xiang G, Xu C, Xu H, Tian N, Zhang X (2019) Carbon monoxide releasing molecule-3 alleviates neuron death after spinal cord injury via inflammasome regulation. EBioMedicine 40:643-654.